Integration of Recognition Elements with Macromolecular Scaffolds: Effects on Polymer Self-Assembly in the Solid State

Roy Shenhar, Amitav Sanyal, Oktay Uzun, Hiroshi Nakade, and Vincent M. Rotello*

Department of Chemistry, University of Massachusetts, Amherst, Massachusetts 01003

Received March 4, 2004; Revised Manuscript Received April 16, 2004

ABSTRACT: Polystyrene scaffolds were grafted with model functionalities featuring strongly interacting hydrogen bonding and aromatic stacking elements. Both glass transition temperatures and degree of microphase separation in functionalized block copolymers depend on the nature of the functionality and in particular on the strength of intermolecular interactions. The polymers under study were amorphous; it was found, however, that domain periodicities of functionalized diblock copolymers in the microphase-separated state are extremely sensitive to local interactions between functionalities and can express even subtle differences in interaction strength. The results emphasize the ability to fine-tune polymer microstructure and thermomechanical behavior using supramolecular chemistry.

Introduction

The ability to synthesize polymers in a controlled or living fashion[1] facilitates the ability to manipulate polymer microstructure, providing a versatile tool for nanotechnology. One prominent example is the phenomenon of microphase separation exhibited by block copolymers, which can be harnessed to create well-defined periodic microdomains of controlled morphologies (e.g., cylinders, spheres, lamellae) on the 10−100 nm scale, a key size scale for emerging technologies.[2] Apart from relative block volumes, a key parameter that can be used to control the size and morphology of the microdomains is the effective incompatibility between the different blocks,[3] which is determined by the essence of comonomers involved.

As the research concerning the solid-state structure of block copolymers deals mainly with polymers that consist of common monomers (e.g., isoprene, styrene, acrylates, and epoxides), the ability to tune the incompatibility as desired is very limited. Polymer functionalization, apart from extending the horizon of polymer properties in general, can offer another handle to control phase architecture by fine-tuning both volume fractions[4] and incompatibility.

Recent studies have demonstrated the ability to use supramolecular chemistry[5] as a novel method for polymer synthesis[6] including creation of special polymeric structures such as block, star, and graft polymers.[7,8] Supramolecular chemistry also affords unique ways for polymer functionalization[9] and facilitates formation of nanoobjects.[4] Polymers modified with recognition units can be used to assemble nanoparticles into discrete structures[10] and for creation of molecularly imprinted sensor matrices.[11] Undoubtedly, the utilization of noncovalent interactions opens new avenues in applied polymer research; nevertheless, while the main attention is being drawn to the constructing abilities of noncovalent interactions, the underlying direct influence of these interactions on the solid-state structure and behavior of amorphous polymers has been little studied to date.[12]

* To whom correspondence should be addressed: Tel (413) 545 2058; Fax (413) 545 4490; e-mail rotello@chem.umass.edu.

In this paper we analyze the effects of recognition units (i.e., units that interact through noncovalent interactions) on solid-state properties of random and block copolymers through a comparison between four different model functionalities: diamidopyridine (DAP), which is capable of molecular recognition through multiple hydrogen bonding interactions, anthracene carboxylate (Anth) and pyrene carboxylate (Pyr), which are capable of aromatic stacking interactions of varying affinity,[13] and diesterpyridine (DEP), offering the weakest intermolecular interaction. In our study, we probed the influence of parameters such as interaction strength and structural rigidity on glass transition temperatures and microphase separation in block copolymers. Our results demonstrate that noncovalent interaction capabilities of side-chain groups impact the physical behavior of polymers in a predictable fashion, providing a versatile and tunable tool for manipulation of polymer properties.

Results and Discussion

Construction of Functionalizable Polymer Scaffolds. Versatile polystyrene scaffolds consisting of styrene and 4-chloromethylstyrene (CMS) comonomers were used for these studies. With these polymers, the chloromethyl groups provide "hooks" for postpolymerization attachment of different functionalities through nucleophilic substitution (Scheme 1). This approach offers two main advantages for investigation of structure−property relationship relative to copolymers composed of very different or prefunctionalized comonomers: (a) using styrene derivatives (i.e., CMS) as the functionalizable monomers in the polystyrene scaffolds enables use of the functionalities as side-chain modifiers to an all-polystyrene backbone, isolating the contribution of the attached functionality to the material properties of the polymer[14] and allowing comparison to the known properties of polystyrene, and (b) it allows true comparison between functionalities while maintaining all parameters pertaining to the polymer (particularly the degree of randomness in the random copolymer/blocks) constant, since the functionalities are grafted to the *exact same* polymer scaffold.

10.1021/ma0495590 CCC: $27.50
Published on Web 06/05/2004

Table 1. Molecular Attributes of Parent P(S-*co*-CMS) and PS-*b*-P(S-*co*-CMS) Polymer Scaffolds

notation	series	M_n (kg/mol)[a] PS[b]	M_n (kg/mol)[a] P(S-*co*-CMS)	M_n (kg/mol)[a] total	PDI[a]	DP[a,c,d]	functionality content (mol %)[a,d,e]
PS/CMS (25, 50%)			24.8	24.8	1.46	194	50
PS/CMS (27:13, 17%)	A	27.3	12.8	40.1	1.26	377	17
PS/CMS (27:13, 25%)	A, B	27.1	12.7	39.8	1.16	370	25
PS/CMS (28:13, 40%)	A	27.8	13.2	41.0	1.25	374	40
PS/CMS (27:20, 25%)	B	27.1	20.1	47.2	1.23	434	25
PS/CMS (27:23, 20%)	B	27.1	23.1	50.2	1.23	464	20
PS/CMS (27:26, 22%)	B	27.1	26.2	53.3	1.25	489	22

[a] According to SEC with PS standards. [b] PDI of all PS blocks were ca. 1.1. [c] Average total degree of polymerization. [d] Calculated from ^{1}H NMR integration. [e] Molar percentage of CMS (in the case of block copolymers represents the percentage within the functionalized block only).

Scheme 1. Schematic Illustration of Postpolymerization Functionalization of a Polystyrene Backbone through Nucleophilic Substitution of Chloride Groups

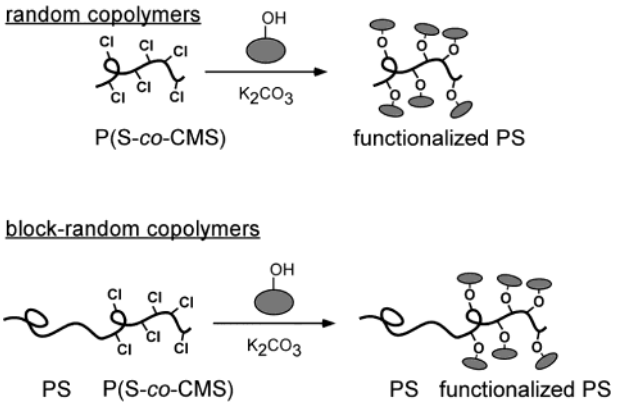

The polymer scaffolds were synthesized through controlled free-radical polymerization using nitroxide initiators,[15] affording relatively narrow polydispersities as well as the ability to create block−random copolymers (which we denote simply as "block copolymers" for brevity). Characteristics of the polymer scaffolds used in this study are summarized in Table 1, and their general structure is depicted in Figure 1 (where R = Cl). The attributes of the scaffolds (i.e., number-averaged molecular weights (M_n) and functionality molar fractions) were also used for the general polymers' notation: PS/X(M_n,z) and PS/X(M_{PS}:$M_{func-PS}$,z) denote polystyrene-based random and diblock copolymers, respectively, which are modified to a molar percentage z with the functionality X.[16] We note that for consistency usage of the term "functionality content" (and analogous terms) when regarding diblock copolymers always refers to the functionality content in the functionalized block only.

The diblock copolymers used in this study form two fundamental series, which we denote A and B (see Table 1), and are meant to probe different characteristics of the microphase separation phenomenon. Series A is comprised of three polymers with compositional characteristics of (27:13,17%), (27:13,25%), and (28:13,40%), in which the molecular weights in both blocks remains constant (±1 kDa) while the functionality content is varied. This series thus allows the investigation of the influence of the functionality content parameter on the effective incompatibility that leads to microphase separation. Series B, on the other hand, consists of four polymers having compositional characteristics of (27:13,25%), (27:20,25%), (27:23,20%), and (27:26,22%), which are all made from the same batch of the first block (PS) and in which the functionality content is very similar. This series therefore allows quantitative probing of the contribution of varying polymer lengths (derived from changes in the functionalized block lengths) to the bulk periodicity of the microphase-separated melts at similar functionality content (vide infra).

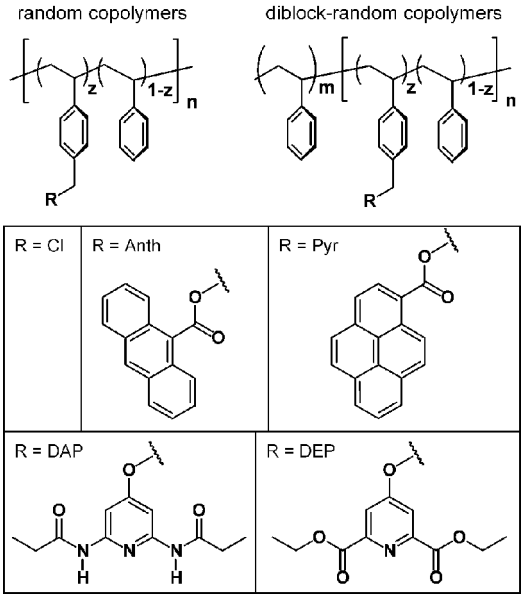

Figure 1. General structure of monoblock and diblock copolymers and model functionalities used in this study. R = Cl corresponds to the parent polymer scaffolds.

Model Functionalities. There are two major factors that affect the solid-state behavior of amorphous polymers: the strength of interaction between polymer segments and structural attributes of the components such as steric bulk and rigidity. The model functionalities used in this study (Figure 1) feature different modes of noncovalent interaction with different degrees of strength while maintaining similar molar volumes (within ±4% of the modified monomer).

As probes for aromatic stacking, we studied 9-anthracene carboxylate (Anth)[17] and 1-pyrene carboxylate (Pyr) (Figure 1). In solution, aromatic stacking of anthracene units was demonstrated to induce a folded chain structure in anthracene-functionalized polystyrenes and enabled hosting electron-poor molecules such as picric acid.[18] Pyrene offers a stronger π-stacking interaction than Anth.[13] Moreover, the excimer emission of pyrene facilitates spectroscopic characterization of the aromatic stacking interaction; ground-state aggregation of pyrene groups in pyrene-functionalized polymers in solution has also been reported.[19,20] Figure 2 shows the fluorescence spectra of solutions and thin films of Pyr-functionalized polystyrenes. All emission spectra are

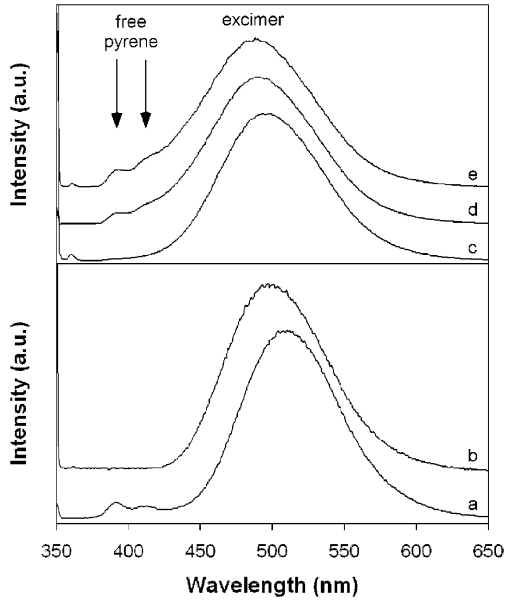

Figure 2. Fluorescence spectra of PS/Pyr (25, 50%) in chloroform solution (a) and as thin film (b) and of thin films of PS/Pyr diblocks of series A with decreasing Pyr content: (c) (28:13, 40%), (d) (27:13, 25%), and (e) (27:13, 17%). The characteristic emission bands of free pyrene and of the excimer have been denoted. Spectra are normalized to the intensity of the excimer peak and are vertically offset for clarity.

dominated by the excimer emission band (at ca. 500−510 nm), which is attributed to formation of ground-state aggregates of the Pyr functionality.[19] Comparison between emission patterns of PS/Pyr(25,50%) in solution and in the solid state (Figure 2a,b) reveals both a blue shift of the excimer emission and disappearance of the emission peaks of free pyrene (at 392 and 412 nm). This indicates, on one hand, enhanced formation of Pyr aggregates and, on the other hand, that the excimer components are improperly oriented in the glassy polymer matrix they are attached to.[21]

The fluorescence from films of the diblock copolymers of PS/Pyr of series A (Figure 2c−e) reveals that decreasing Pyr content results in a further blue shift of the excimer peak and an increase in the relative intensity of the free pyrene emission. This corroborates the previous result, as it is to be expected that in glassy polymer matrices with smaller density of functionality the statistical chance to form dimers decreases (hence the intensification in the free pyrene emission bands) and that the dimers formed would be more spatially constrained and therefore improperly oriented than in polymers with higher functionality content (hence the blue shift in the excimer emission).[21]

Hydrogen bonding was explored using 2,6-diacyldiamidopyridine (DAP) (Figure 1), which is of general interest due to its ability to form host−guest recognition dyads through three-point hydrogen bonding with complementary groups such as uracils.[9,22] In terms of self-interaction, the hydrogen donor−acceptor−donor arrangement existing in DAP enables DAP−DAP dimerization through two-point hydrogen bonding (Figure 3).[23] While in solution such dimerization is weak [$K_{dim} \sim 10^{-1}$ M^{-1} in chloroform as known from NMR titration studies[24] and also as evidenced by the single, sharp N−H stretching mode at 3424 cm^{-1} exhibited by the analogous 4-benzyloxy-3,5-dipropamidopyridine (Bz-DAP), Figure 4], hydrogen bonding is prominent in the solid state. The infrared spectra of solid samples of

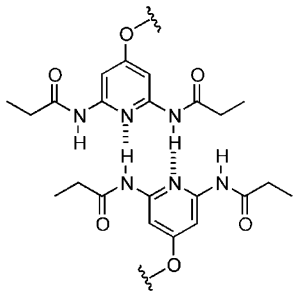

Figure 3. Preferred dimerization arrangement of DAP through two-point hydrogen bonding.[23]

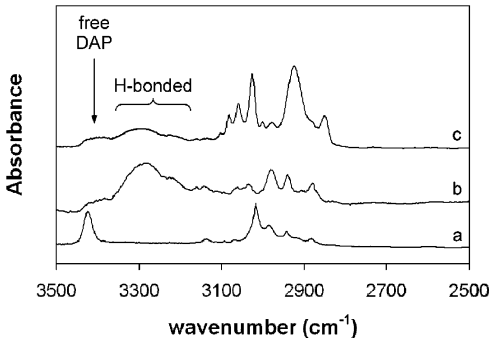

Figure 4. Infrared spectra showing N−H and C−H stretching modes: (a) Bz-DAP in chloroform solution and (b) in the solid state, (c) solid PS/DAP(28:13, 40%). The free N−H stretch and the hydrogen-bonded N−H stretching region have been denoted. Spectra are offset for clarity.

both Bz-DAP and PS/DAP(28:13,40%) (a representative DAP-functionalized polymer) exhibit multiple, broad, and red-shifted N−H stretching modes at 3290−3300 cm^{-1} (Figure 4), which are attributed to hydrogen-bonded N−H groups.[11b] One of our goals was to probe the influence of this dimerization interaction on the polymer structure and thermal behavior[12] and to gain insight into the role of hydrogen bonding in these systems by comparison to other model functionalities.

The analogous 2,6-diesterpyridine (DEP) was used as control for DAP (Figure 1). DEP is highly analogous in structure to DAP but can only interact with other DEP functionalities through dipolar interactions, making it closer in interaction strength to Anth and Pyr. It should be noted, that despite the similarity in volumes between all four functionalities, DEP and DAP are much more flexible entities than the polycyclic Anth and Pyr. This, therefore, makes DEP a useful "yardstick" by which each observed effect could be attributed either to the strength of interaction or to structural rigidity based on comparison to DAP, Anth, and Pyr.

Glass Transition Temperature. Among the most important, complex, and unsolved physical problems in material science is the glass transition phenomenon, which is the thermal transition in polymers from the hard glassy state to the soft rubbery state.[25] Technologically, the glass transition is of crucial importance, as it dictates thermomechanical behavior and hence processing conditions (e.g., molding temperatures). In block copolymers, overcoming the glass transition temperature (either by thermal annealing or by solvent plasticization) is required in order to enable relaxation into the thermodynamically stable, microphase-separated structure and to eliminate structural defects.

In the simplified description of the phenomenon, the glass transition occurs when a certain "free volume" is reached that allows freedom of motion for the chain

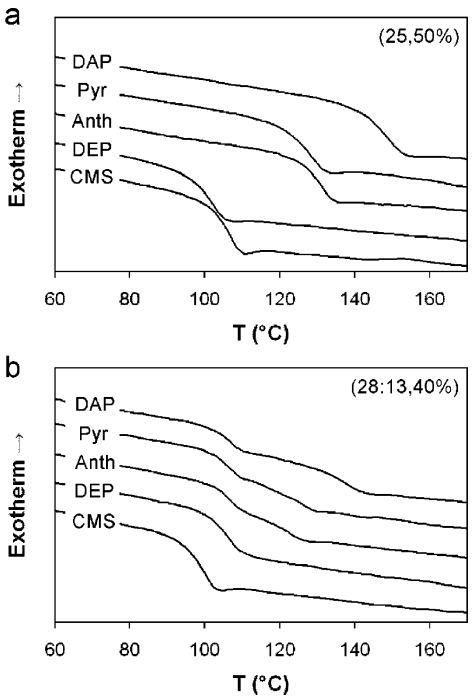

Figure 5. DSC scans of PS/CMS, PS/DEP, PS/Pyr, PS/Anth, and PS/DAP: (a) (25, 50%) random copolymers and (b) (28: 13, 40%) diblock copolymers.

segments and thus enables execution of cooperative motions. There are two main factors that dominate the glass transition phenomenon: cohesive forces and chain stiffness.[26] With regard to the polymers discussed in this paper, noncovalent interactions give rise to increased cohesion between chains.[8,27] Additionally, bulky and rigid side-chain groups, which substantially increase the barrier for rotation, increase chain stiffness and hence are expected to increase the glass transition temperature (T_g).[28]

Figure 5a shows differential scanning calorimetry (DSC) scans obtained for the random copolymer scaffold PS/CMS(25,50%) and the corresponding functionalized polymers PS/DEP, PS/Anth, PS/Pyr, and PS/DAP, for which glass transition temperatures of 107, 102, 131, 128, and 149 °C, respectively, are measured. While the PS/CMS scaffold and the polymer modified with the DEP functionality show T_g's that are similar to that of PS (100 °C),[29] those corresponding to PS/Pyr, PS/Anth, and PS/DAP are substantially higher.

The weak effect on glass transition temperature induced by functionalization with DEP indicates both weak interaction between DEP units and a small contribution to the overall chain stiffness, with an additional plasticization effect induced by the flexible alkyl substituents. As DAP is structurally very similar to DEP, the largest effect observed with PS/DAP must therefore be associated mainly with its ability to interact through hydrogen bonding, which enhances overall cohesion between the chains. In contrast, the increased T_g's observed for PS/Pyr and PS/Anth probably arise from both cohesive forces and chain stiffness. Increased cohesion in PS/Anth and PS/Pyr arises from aromatic stacking between the functionalities (accounted for by the fluorescence spectra of PS/Pyr films shown above) and possibly also from stacking interactions between the functionality and phenyl rings in the PS chains. The structural rigidity of the Anth and Pyr units, on the other hand, is expected to impart additional chain stiffness, which also contributes to an increased T_g.

In block copolymers that have the composition (28: 13,40%), where the functionalized blocks feature functionality content that is only slightly lower than that of the previously described random copolymers (25,50%), the increased T_g's of the functionalized blocks imparted by the Pyr, Anth, and DAP functionalities result in two distinct transitions (Figure 5b). This situation clearly indicates microphase separation in those polymers, where the PS domains soften at 106−107 °C and Anth-, Pyr-, and DAP-functionalized-PS domains become rubbery at 125, 126, and 139 °C, respectively.[30] This does not imply that the diblock copolymers of PS/DEP or even PS/CMS do not microphase separate upon annealing (as will be seen later, PS/DEP(28:13,40%) does create a microphase-separated structure); it demonstrates, however, that distinction in the thermomechanical behavior between the PS and the functionalized-PS domains cannot be achieved using DEP, while it can be readily obtained using functionalities that are capable of noncovalent interactions. The distinction between the thermomechanical properties of PS and functionalized-PS domains in PS/Anth, PS/Pyr, and PS/DAP makes these materials thermoplastic elastomers;[12] i.e., materials that can be repeatedly softened under the application of heat (thermoplastic behavior) and upon cooling to temperatures between the T_g's of the PS and functionalized-PS domains retain elastic properties similar to cross-linked elastomers due to the "physical cross-linking" of the rubbery (PS) domains by the glassy (functionalized-PS) domains.

Microphase Separation in Block Copolymers. The physical origin of microphase separation in block copolymers is the incompatibility between different polymer segments.[31] The covalent bond connecting between the polymer blocks prevents phase separation on a macroscopic length scale; coupling this property with the tendency to reduce interfacial area between the distinct polymer domains (phases) gives rise to periodic microdomains with tuned morphology (e.g., lamellae, cylinders, spheres), which is controlled through both the block volume fractions and the degree of incompatibility.[3]

The incompatibility between blocks A and B in a diblock copolymer PA-*b*-PB is quantified by the Flory−Huggins interaction parameter χ_{AB}, which is a dimensionless parameter that can be expressed in terms of attractive energy elements as follows:[32]

$$\chi_{AB} \propto (\epsilon_{AA} + \epsilon_{BB} - 2\epsilon_{AB})/2kT \qquad (1)$$

where ϵ_{AA} and ϵ_{BB} describe the attraction between polymer segments of the same type (that favor phase separation), ϵ_{AB} represents the attraction between the two types of segments (and is thus related to the enthalpic gain from mixing), and k and T are the Boltzmann constant and the absolute temperature, respectively. In block copolymer systems that exhibit phase separation (i.e., where no strong attraction exists between the two blocks to overwhelm the mixing preference of like segments), the value of χ is positive. In the context of this paper, functionalizing block B, for instance, with units that interact with each other will mainly affect the term ϵ_{BB} by increasing its value, which in turn results in an overall increase of the incompatibility between the blocks.

Table 2. Domain Periodicities and Molecular Attributes of the Functionalized Diblock Copolymers

composition	series		$N^{a,b}$	$x^{b,c}$	$f^{b,d}$	a (Å)	D (nm)[e]	morphology[f]
(27:13, 17%)	A	DEP	416	0.38	0.37	6.8	23.2	
		Anth	412	0.36	0.36	6.8		
		Pyr	415	0.37	0.37	6.8	23.6	
		DAP	417	0.39	0.37	6.8	27.5	
(27:13, 25%)	A,B	DEP	426	0.50	0.39	6.8	23.0	
		Anth	420	0.49	0.38	6.8	22.8	
		Pyr	425	0.50	0.39	6.9	23.9	
		DAP	428	0.51	0.39	6.8	26.9	lamellar
(28:13, 40%)	A	DEP	463	0.67	0.42	6.8	27.9	
		Anth	453	0.65	0.41	6.9	28.7	lamellar
		Pyr	460	0.67	0.42	6.9	30.2	lamellar
		DAP	466	0.68	0.43	6.8	34.8	lamellar
(27:20, 25%)	B	DEP	523	0.50	0.50	6.8	26.5	
		Anth	514	0.49	0.49	6.8	25.4	
		Pyr	520	0.50	0.50	6.8	27.4	lamellar
		DAP	526	0.51	0.50	6.8	31.4	lamellar
(27:23, 20%)	B	DEP	548	0.43	0.52	6.8	26.6	
		Anth	539	0.42	0.52	6.8	26.1	
		Pyr	545	0.43	0.52	6.8	28.0	lamellar
		DAP	551	0.44	0.53	6.8	32.5	lamellar
(27:26, 22%)	B	DEP	594	0.47	0.56	6.8	27.8	
		Anth	582	0.45	0.55	6.8	27.2	
		Pyr	590	0.46	0.56	6.8	29.2	lamellar
		DAP	597	0.47	0.56	6.8	33.7	lamellar

[a] Volume-effective degree of polymerization (using PS repeat unit as the reference volume). [b] Calculated from M_n values of corresponding PS/CMS scaffolds, functionality content, and the respective calculated molar volumes of styrene and functionalized styrene (see Experimental Section). [c] Volume fraction of the functionality in the functionalized block (i.e., volume-corrected functionality content). [d] Volume fraction of the functionalized blocks. [e] Calculated from Lorentz-corrected intensity (q^2I vs q) plots (assuming lamellar morphology based on volume fractions). [f] Determined from relative location of secondary maxima in the SAXS curves with respect to the first Bragg reflection.

As the diblock copolymers under investigation are not pure block copolymers but rather block−random copolymers, the effective incompatibility (χ_{eff}) varies with the volume fraction of the functionality in the functionalized block (x) as follows:[33]

$$\chi_{eff} = x^2 \chi_{S,S-X} \tag{2}$$

where S-X denotes styrene modified with the functionality X. The effective incompatibility can be estimated from the domain periodicity (D) of the microphase-separated bulk, calculated from the first Bragg reflection in the small-angle X-ray scattering (SAXS) curve. According to Vavasour and Whitmore, the periodicity scales with the effective incompatibility and the effective degree of polymerization (N) as follows:[34]

$$D \propto a\chi_{eff}{}^{p} N^{p+1/2} \tag{3}$$

where a is the average statistical segment length (calculated with respect to a reference monomer volume). The scaling power p changes with the degree of microphase separation (quantified by the product $\chi_{eff}N$). While in the disordered state $p = 0$ (the characteristic length scale is $1.318aN^{1/2}$, reflecting Gaussian chain statistics),[35] immediately after crossing the critical point the exponent jumps to ~0.5,[36,37] and as the degree of microphase separation increases, it gradually decreases and levels off at the strong segregation limit (SSL, $\chi_{eff}N > 100$) at $p = {}^1/_6$.[38] The exact expression for the lamellar structure in the SSL originally derived by Semenov,[39] which is in agreement with other segregation theories[40] and with experiment,[41] is given in eq 4.

$$D = 1.10a\chi_{eff}{}^{1/6} N^{2/3} \tag{4}$$

Matsen and Bates compared the prediction of D from self-consistent mean-field theory with values that are obtained by extrapolation of the strong segregation theory (eq 4) to the weak segregation limit (WSL).[36] While the results differ by about 20% when $\chi_{eff}N = 10$, this different rapidly decreases at higher segregation strengths (e.g., 5% at $\chi_{eff}N = 40$). Therefore, for practical purposes, the use of eq 4 can be extended within reasonable accuracy into the intermediate segregation regime.[42] For block copolymers that feature weaker segregation, a refinement that employs eq 3 with an intermediate exponent value ($0.17 < p < 0.50$) should give a reasonable and internally consistent estimate of χ_{eff}.

Equations 1−4 set the theoretical framework for an investigation of the effect of noncovalent interactions on microphase-separated structures in the functionalized block copolymers under study.[12c] The molecular characteristics and the calculated domain periodicities of the functionalized diblock copolymers are summarized in Table 2.

Figure 6 shows the SAXS curves of polymers of series A functionalized with either one of the four functionalities. Throughout this series, the respective volumes of the PS block and of the functionalized-PS block as well as the effective degrees of polymerization are very similar while the functionality content is varied between 17% and 40%. At the lowest functionality content (17%), the SAXS profiles of PS/DEP, PS/Anth, and PS/Pyr exhibit either a broad scattering peak (PS/DEP and PS/Pyr) or no reflections at all (PS/Anth), evidencing very low incompatibility between the functionalized block and the PS block in these polymers.[43] PS/DAP, in contrast, is clearly microphase-separated, indicating a larger value of $\chi_{S,S-DAP}$. As the functionality molar fraction is raised to 25% and 40%, all polymer samples exhibit scattering peaks that are shifted toward low angles (corresponding to larger periodicities) in accordance with increased incompatibility (eqs 2 and 3). Dimerization of the DAP units through the relatively

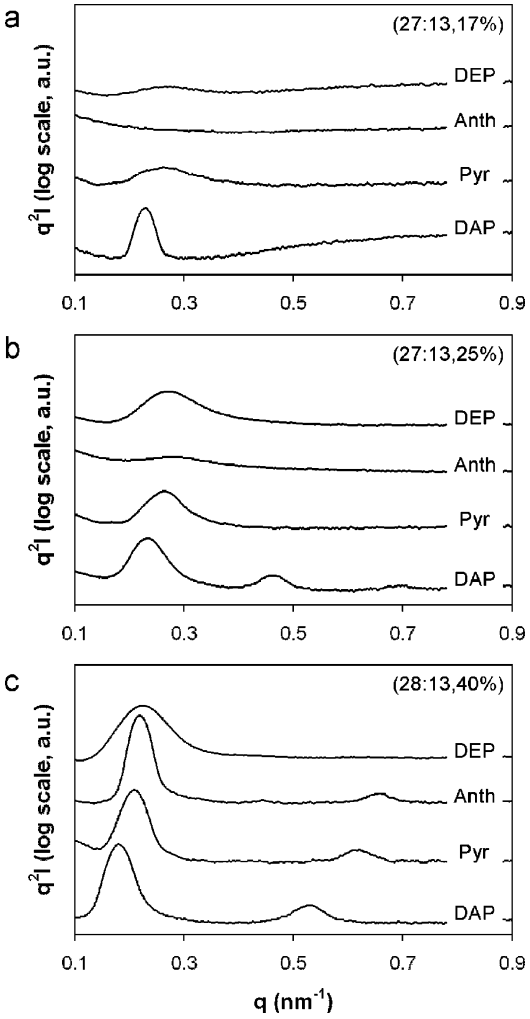

Figure 6. SAXS profiles of polymers of series A functionalized with DEP, Anth, Pyr, and DAP functionalities: (a) (27:13, 17%), (b) (27:13, 25%), (c) (28:13, 40%). Curves are offset for clarity.

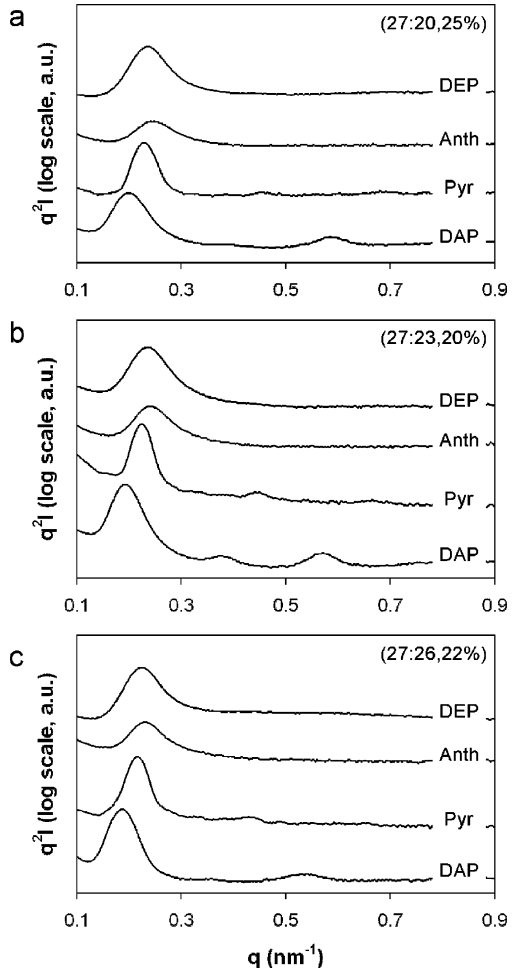

Figure 7. SAXS profiles of polymers of series B functionalized with DEP, Anth, Pyr, and DAP functionalities: (a) (27:20, 25%), (b) (27:23, 20%), (c) (27:26, 22%). Curves are offset for clarity.

strong multiple hydrogen-bonding interactions results in the largest incompatibility between the functionalized block and the PS block in PS/DAP polymers, as manifested by the largest periodicities measured among the four functionalities as well as an appearance of higher order reflections already at low functionality content (e.g., 25%). Appearance of higher order reflections indicates enhanced ordering of the domains and the scattering pattern (i.e., location of the secondary maxima in relation to that of the first Bragg reflection q^*) enables determination of the morphology. In qualitative agreement with our estimation of volume fractions, PS/DAP(27:13,25%) ($f_{\text{func-PS}} = 0.39$) exhibits thickness-asymmetric lamellae, while the functionalized polymers of the (28:13,40%) composition ($f_{\text{func-PS}} = 0.41-0.43$), which exhibit volume fractions of the functionalized block that are closer to $f = 0.5$, reveal close-to-symmetric lamellar morphology (as indicated by the attenuation of the second-order peak at $2q^*$).

Each quartet of functionalized polymers that originate from the same scaffold features almost identical molecular parameters (i.e., volume fractions and effective degrees of polymerization). As such, the periodicity serves as a measure for the degree of interaction afforded by the corresponding functionality. It is important to note that despite the fundamental structural difference between DEP and Anth, polymers functionalized with these units show very similar periodicities in the microphase-separated samples, indicating similar incompatibility values (i.e., $\chi_{\text{S,S-Anth}} \cong \chi_{\text{S,S-DEP}}$). Functionalization with Pyr, featuring enhanced aromatic stacking capability (compared to that of Anth),[13] leads to an even higher incompatibility, and as mentioned above, the much stronger hydrogen-bonding interactions in PS/DAP polymers lead to a significant enhancement in the degree of microphase separation.

To obtain a quantitative evaluation of the incompatibility for each of the functionalities, we employed the polymers of series B. The polymers in this series are highly analogous[44] and feature a relatively low and fairly uniform functionality content; this is crucial for the reference to the functionalized blocks as random copolymers and allows, to a reasonable approximation, modeling the scaling of the periodicity with N according to the same power law (eq 3) for each of the functionalities.[45]

Figure 7 shows the SAXS profiles of the three longest polymers of series B, where the qualitative order of $\chi_{\text{S,S-DEP}} \cong \chi_{\text{S,S-Anth}} < \chi_{\text{S,S-Pyr}} \ll \chi_{\text{S,S-DAP}}$ can clearly be estimated from the positions of the first Bragg reflections and the existence of higher order reflections. As PS/DAP polymers feature the highest degree of segregation, eq 4 should be more accurately applicable to them than to polymers functionalized with the other functionalities. The average value of $\chi_{\text{S,S-DAP}}$ calculated

Table 3. Average Incompatibility and Segregation Strength Values Calculated Using $\chi_{S,S-dap} = 0.31$ and Eq 3 with Different Exponent p Values and Incompatibility Values Obtained from Semiempirical Calculations[46]

		PS/DEP	PS/Anth	PS/Pyr
$p = 0.17$ (SSL)	$\chi_{S,S-X}$	0.11 ± 0.01	0.11 ± 0.01	0.14 ± 0.02
	$\chi_{eff}N$ range	11−14	11−12	13−17
$p = 0.20$	$\chi_{S,S-X}$	0.13 ± 0.02	0.13 ± 0.02	0.16 ± 0.03
	$\chi_{eff}N$ range	13−17	12−15	15−20
$p = 0.25$	$\chi_{S,S-X}$	0.15 ± 0.02	0.16 ± 0.02	0.19 ± 0.03
	$\chi_{eff}N$ range	15−20	15−18	17−23
$p = 0.30$	$\chi_{S,S-X}$	0.17 ± 0.03	0.18 ± 0.03	0.20 ± 0.04
	$\chi_{eff}N$ range	16−22	16−21	18−25
$p = 0.50$ (WSL)	$\chi_{S,S-X}$	0.22 ± 0.04	0.23 ± 0.04	0.25 ± 0.05
	$\chi_{eff}N$ range	20−28	20−27	22−31
topological indices[26]	$\chi_{S,S-X}$	0.09	0.10	0.13

using eqs 2 and 4 is 0.31 ± 0.06,[46] locating the PS/DAP polymers of series B in the segregation region between $\chi_{eff}N = 28$ and 42.

Once the value of $\chi_{S,S-DAP}$ has been determined and the segregation strength of the PS/DAP polymers of series B were located in the intermediate segregation regime, the other incompatibility values can be calculated relative to $\chi_{S,S-DAP}$ using eq 3 with different exponent values that are typical to the intermediate segregation regime. Table 3 summarizes the averaged calculated incompatibility values of PS/DEP, PS/Anth, and PS/Pyr and provides a comparison between five exponent values spanning the range from 0.17 to 0.50 (SSL to WSL, respectively). The respective $\chi_{eff}N$ values were also calculated to probe the validity of usage of the different exponent values.

The data summarized in Table 3 indicate that assuming either of the extreme cases (WSL or SSL) for the PS/DEP, PS/Anth, and PS/Pyr polymers of series B locates them in segregation strength ranges that are inconsistent with the assumption being made (i.e., assuming SSL results in $\chi_{eff}N$ values in the range 11−17, which are in the WSL and, conversely, assuming WSL locates the polymers well into the intermediate segregation regime, where scaling of $p = 0.5$ is unjustified). Such assumptions are expected to yield large deviations from the true incompatibility values. Intermediate exponent values (e.g., $p = 0.25-0.30$) give a more consistent picture and associate these polymers with the intermediate segregation regime as expected from the qualitative experimental observations (e.g., existence of higher order reflections). Such scaling exponents are in accordance with the experimental results of others (where periodicity was found to depend of $N^{0.8}$ in the intermediate segregation regime)[45] and our observation that the SAXS curves of these polymers do not exhibit strong temperature dependence (as would be expected from polymer bordering the order−disorder transition[45a]).

Although a few assumptions were involved in the determination of the incompatibility values, we estimate that our results are accurate within 25%. Even within this error, a clear trend is observed, where functionalization with DEP or Anth yields a moderate incompatibility, modification with Pyr results in a slightly increased incompatibility, and attaching DAP functionalities to the polystyrene backbone almost doubles the incompatibility compared to polymers functionalized with DEP or Anth. Values obtained from semiempirical calculations (Table 3) reproduce the same trend (apart from an apparent overestimation of the hydrogen-bonding effect on the incompatibility in PS/DAP).[46]

Both experimental and theoretical values point to an apparent correlation between the mode and the strength of noncovalent interaction and the incompatibility imparted on the polymer segments, where multiple hydrogen-bonding interactions have greater impact than aromatic stacking interactions. It is important to note that, even within the class of aromatic stacking interactions, domain periodicities are very sensitive to the strength of the interactions, where the stronger dimerization tendency of Pyr over Anth[13] translates to 20−25% increase in the determined incompatibility between S-Pyr with styrene compared to that of S-Anth with styrene.

Conclusions

A series of polymer scaffolds based on styrene and 4-chloromethylstyrene were functionalized with four model functionalities, each featuring a unique combination of structural and chemical properties with emphasis being given to molecular recognition capability. Characterization using thermal analysis and X-ray scattering revealed a distinct behavior pattern for each system: the glass transition depends on both structure and interaction capability, while microphase separation in functionalized diblock copolymers is determined mainly by the interaction strength and is highly sensitive to subtle changes.

Our findings demonstrate that molecular recognition units attached to polymers can be used to control the solid-state structure and behavior of polymers. The results presented in this paper clearly demonstrate the ability to integrate molecular chemistry with solid-state polymer physics for the prediction and manipulation of material properties starting at the molecular level. The approach used in this study is general (i.e., can be applied to a wide variety of functionalities available through organic synthesis) and can be further utilized for the study of structure−property relationship in polymer science. This study, thus, also lays the foundation for the fundamental analysis of systems that integrate supramolecular chemistry and polymers.

Experimental Section

Materials. All chemicals were reagent grade, purchased from Aldrich or Merck with the exception of chelidamic acid (TCI America), and were used as received. Monomers (styrene and 4-chloromethylstyrene) were purified from the inhibitor using a short alumina plug.

Synthesis. P(S-*co*-CMS) and PS-*b*-P(S-*co*-CMS) polymer scaffolds were synthesized via nitroxide-mediated controlled radical polymerization.[15] In the case of diblock copolymers, the PS block was created first, purified by precipitation in methanol from remaining monomer, and then polymerization of the S/CMS mixture to yield the functionalizable block took place. Polymerizations of the functionalizable block were stopped at less than 10% conversion to decrease the possibility of blocki-

ness that may arise from the different reactivity ratios of styrene and CMS (0.62 and 1.12, respectively).[29]

2,6-Dipropamidopyrid-4-one (DAP). The compound was synthesized as previously published.[47]

2,6-Diethylchelidamate (DEP). The compound was synthesized according to the literature procedure.[48] Chelidamic acid (0.5 g) was refluxed in 2% sulfuric acid in ethanol overnight, concentrated in vacuo, dissolved in water, and extracted twice with dichloromethane. Column chromatography (SiO_2, 1:1 ethyl acetate:hexanes) provided 314 mg (53%) of the titled compound as a white crystalline solid; mp 118−120 °C (lit.[48] 120−121 °C).

Polymer Functionalization. In a typical functionalization reaction, the parent polymer (50 mg), the functionality (1.1 CMS equiv), and K_2CO_3 (1.5 CMS equiv) were dissolved in 2 mL of *N*,*N*-dimethylformamide (DMF) and stirred at 70 °C under an argon atmosphere overnight. Dropwise addition of water resulted in immediate precipitation. The solid was briefly sonicated in 15 mL of water, filtered, sonicated in 15 mL of methanol, filtered again, and dried under vacuum overnight (70−90% yield). Complete conversion (within NMR detection limits) was determined using the side-chain CH_2 group resonance.

Characterization. Number-averaged molecular weights (M_n) and polydispersity indices (PDI) of the polymers in THF solutions were determined from gel permeation chromatograms (GPC) acquired on an in-house built GPC system using PL Caliber data collection software, three-column set (Polymer Labs, Inc.; PLgel 5 μm columns, 300 × 7.5 mm, 10^3, 10^4, and 10^5 Å pore size), with an RI detector (Waters 403). The system was calibrated with respect to polystyrene standards (Polymer Labs, Inc.). CMS content was calculated according to ^{1}H NMR peak integration (using a Bruker AC-200 spectrometer operating at 200.13 MHz for ^{1}H) to an estimated error of ±5% CMS content. NMR spectra were taken in $CDCl_3$, except from PS/DAP(25,50%) which was measured in DMSO-d_6. Glass transition temperatures were determined using differential scanning calorimetry (DSC), performed on ca. 10 mg samples under continuous nitrogen purge (50 mL/min) on a TA Instruments DSC 2910. Data represent the second heating cycles using a heating scan rate of 10 °C/min. Infrared spectra were recorded using either KBr plates or a solution cell on a MIDAC 2000 FTIR spectrometer. Fluorescence spectra of dilute solutions (in a 1 mm quartz cuvette) or of thin films (deposited from solution onto glass slides and annealed at 150 °C for 2 h) were acquired on a Shimadzu RF-5301 PC spectrofluorophotometer. Samples were excited at 350 nm.

Small-Angle X-ray Scattering (SAXS). To avoid kinetic entrapment by solvent evaporation effects, solid polymer samples (ca. 10 mg) in the precipitated powder form were annealed at 150 °C under vacuum for 2 days and quenched to room temperature. Cu Kα X-rays (1.54 Å) were generated in an Osmic MaxFlux source with a confocal multilayer optic (OSMIC, Inc.). Images were taken with a Molecular Metrology, Inc., camera consisting of a three pinhole collimation system, 150 cm sample-to-detector distance (calibrated using silver behenate), and a 2-dimensional, multiwire proportional detector (Molecular Metrology, Inc.). The entire X-ray path length was evacuated from the optic to the detector in order to reduce the background from air scattering. This setup allowed neglecting the correction for background scattering as proved by experiment. Two-dimensional images were reduced to the one-dimensional form using angular integration. Scattering vectors (q) were calculated from the scattering angles (θ) using $q = 4\pi \sin\theta/\lambda$, and domain periodicities (D) were calculated from Gaussian fits to the principal scattering maxima of the Lorentz-corrected intensities using $D = 2\pi/q$.

Semiempirical Calculations. All molar and van der Waals volumes (of the modified styrene monomers as well as that of styrene) were calculated using topological indices,[26] a method that is derived from graph theory and is considered to give remarkably reliable predictions due to the excellent correlation ($R^2 = 0.998$) found with experimental values. Mass densities of the homopolymers of PS/Pyr, PS/Anth, PS/DEP, and PS/DAP calculated from the molar volumes are 1.247, 1.227, 1.196, and 1.163 g/mL, respectively. Effective degrees of polymerization (N), statistical segment lengths (a), and volume fractions (f and x parameters) were referenced to a constant monomer volume of styrene as calculated using topological indices ($v_0 = 161.03$ Å^3), which is reasonably close to that calculated from the experimental density (164.48 Å^3).[29] Using 6.7 Å as the statistical segment length of styrene (a_S)[28] in combination with the corresponding calculated densities, we estimated 7.2 Å for a_{S-Anth} and a_{S-Pyr} and 7.1 and 7.0 Å for a_{S-DEP} and a_{S-DAP}, respectively.[17,49] The average statistical segment length was then calculated according to the following relationship:[42]

$$a = \left(\frac{1-f}{a_S^2} + \frac{f}{x a_{S-X}^2 + (1-x)a_S^2}\right)^{-1/2}$$

For comparison with experimental results, interaction parameters were calculated from cohesive energies that were also calculated using the topological indices methods, which exhibit $R^2 = 0.995$ correlation with experimental values.[26]

Acknowledgment. R.S. is in debt to Prof. Marc A. Hillmyer, Prof. Thomas P. Russell, and Matthew J. Misner for helpful discussions and assistance. Financial support from the NSF [CHE-0213354 (V.R.)] and MRSEC (DMR 0213695) is gratefully acknowledged. R.S. thanks The Fulbright Foundation for a postdoctoral fellowship.

Supporting Information Available: GPC traces and NMR spectra of all discussed polymers. This material is available free of charge via the Internet at http://pubs.acs.org.

References and Notes

(1) See, for example: Szwarc, M.; van Beylen, M. *Ionic Polymerization and Living Polymers*; Chapman & Hall: New York, 1993. Trnka, T. M.; Grubbs, R. H. *Acc. Chem. Res.* **2001**, *34*, 18.

(2) Thurn-Albrecht, T.; Schotter, J.; Kästle, C. A.; Emley, N.; Shibauchi, T.; Krusin-Elbaum, L.; Guarini, K.; Black, C. T.; Tuominen, M. T.; Russell, T. P. *Science* **2000**, *290*, 2126. Chan, V. Z.-H.; Hoffman, J.; Lee, V. Y.; Iatrou, H.; Avgeropoulos, A.; Hadjichristidis, N.; Miller, R. D.; Thomas, E. L. *Science* **1999**, *286*, 1716. Park, M.; Harrison, C.; Chaikin, P. M.; Register, R. A.; Adamson, D. H. *Science* **1997**, *276*, 1401.

(3) Fredrickson, G. H.; Bates, F. S. *Annu. Rev. Mater. Sci.* **1996**, *26*, 501. Bates, F. S.; Fredrickson, G. H. *Annu. Rev. Phys. Chem.* **1990**, *41*, 525.

(4) Ruokolainen, J.; Mäkinen, R.; Torkkeli, M.; Mäkelä, T.; Serimaa, R.; ten Brinke, G.; Ikkala, O. *Science* **1998**, *280*, 557. Ikkala, O.; ten Brinke, G. *Science* **2002**, *295*, 2407.

(5) Grzybowski, B.; Whitesides, G. M. *Science* **2002**, *295*, 2418. Lehn, J.-M. *Supramolecular Chemistry, Concepts and Perspectives*; VCH: Weinheim, Germany, 1995. Whitesides, G. M.; Mathias, J. P.; Seto, C. T. *Science* **1991**, *254*, 1312. Whitesides, G. M.; Simanek, E. E.; Mathias, J. P.; Seto, C. T.; Chin, D. N.; Mammen, M.; Gordon, D. M. *Acc. Chem. Res.* **1995**, *28*, 37. Stupp, S. I.; LeBonheur, V.; Walker, K.; Li, L. S.; Huggins, K. E.; Keser, M.; Amstutz, A. *Science* **1997**, *276*, 384.

(6) Sijbesma, R. P.; Beijer, F. H.; Brunsveld, L.; Folmer, B. J. B.; Hirschberg, J. H. K. K.; Lange, R. F. M.; Lowe, J. K. L.; Meijer, E. W. *Science* **1997**, *278*, 1601. Keizer, H. M.; Sijbesma, R. P.; Jansen, J. F. G. A.; Pasternack, G.; Meijer, E. W. *Macromolecules* **2003**, *36*, 5602. Hirschberg, J. H. K. K.; Brunsveld, L.; Ramzi, A.; Vekemans, J. A. J. M.; Sijbesma, R. P.; Meijer, E. W. *Nature (London)* **2000**, *407*, 167. Folmer, B. J. B.; Sijbesma, R. P.; Versteegen, R. M.; van der Rijt, J. A. J.; Meijer, E. W. *Adv. Mater.* **2000**, *12*, 874. Lange, R. F. M.; Van Gurp, M.; Meijer, E. W. *J. Polym. Sci., Polym. Chem.* **1999**, *37*, 3657. Lange, R. F. M.; Meijer, E. W. *Macromolecules* **1995**, *28*, 782. Zubarev, E. R.; Pralle, M. U.; Li, L. M.; Stupp, S. I. *Science* **1999**, *283*, 523. Zubarev, E. R.; Pralle, M. U.; Sone, E. D.; Stupp, S. I. *Adv. Mater.* **2002**, *14*, 198.

(7) Gohy, J. F.; Lohmeijer, B. G. G.; Schubert, U. S. *Chem.—Eur. J.* **2003**, *9*, 3472. Lohmeijer, B. G. G.; Schubert, U. S. *J. Polym. Sci., Polym. Chem.* **2003**, *41*, 1413. Meier, M. A. R.;

Lohmeijer, B. G. G.; Schubert, U. S. *Macromol. Rapid Commun.* **2003**, *24*, 852. Gohy, J. F.; Lohmeijer, B. G. G.; Varshney, S. K.; Schubert, U. S. *Macromolecules* **2002**, *35*, 7427. Yamauchi, K.; Lizotte, J. R.; Long, T. E. *Macromolecules* **2003**, *36*, 1083. Yamauchi, K.; Lizotte, J. R.; Hercules, D. M.; Vergne, M. J.; Long, T. E. *J. Am. Chem. Soc.* **2002**, *124*, 8599. Yamauchi, K.; Lizotte, J. R.; Long, T. E. *Macromolecules* **2002**, *35*, 8745.

(8) Yamauchi, K.; Lizotte, J. R.; Long, T. E. *Macromolecules* **2003**, *36*, 1083. Yamauchi, K.; Lizotte, J. R.; Hercules, D. M.; Vergne, M. J.; Long, T. E. *J. Am. Chem. Soc.* **2002**, *124*, 8599. Yamauchi, K.; Lizotte, J. R.; Long, T. E. *Macromolecules* **2002**, *35*, 8745.

(9) Pollino, J. M.; Stubbs, L. P.; Weck, M. *J. Am. Chem. Soc.* **2004**, *126*, 563. Stubbs, L. P.; Weck, M. *Chem.—Eur. J.* **2003**, *9*, 992.

(10) Boal, A. K.; Ilhan, F.; DeRouchey, J. E.; Thurn-Albrecht, T.; Russell, T. P.; Rotello, V. M. *Nature (London)* **2000**, *404*, 746. Frankamp, B. L.; Uzun, O.; Ilhan, F.; Boal, A. K.; Rotello, V. M. *J. Am. Chem. Soc.* **2002**, *124*, 892.

(11) Das, K.; Penelle, J.; Rotello, V. M. *Langmuir* **2003**, *19*, 3921. Duffy, D. J.; Das, K.; Hsu, S. L.; Penelle, J.; Rotello, V. M.; Stidham, H. D. *J. Am. Chem. Soc.* **2002**, *124*, 8290.

(12) (a) Chino, K.; Ashiura, M. *Macromolecules* **2001**, *34*, 9201. (b) de Lucca Freitas, L.; Jacobi, M. M.; Gonçalves, G.; Stadler, R. *Macromolecules* **1998**, *31*, 3379. (c) de Lucca Freitas, L. L.; Stadler, R. *Macromolecules* **1987**, *20*, 2478.

(13) Gonzalez, C.; Lim, E. C. *J. Phys. Chem. A* **2003**, *107*, 10105.

(14) For an example where an attached mesogen creates a sense of a diblock copolymer, see: Sentenac, D.; Demirel, A. L.; Lub, J.; de Jeu, W. H. *Macromolecules* **1999**, *32*, 3235.

(15) Benoit, D.; Chaplinski, V.; Braslau, R.; Hawker, C. J. *J. Am. Chem. Soc.* **1999**, *121*, 3904. Harth, E.; Hawker, C. J.; Fan, W.; Waymouth, R. M. *Macromolecules* **2001**, *34*, 3856. Hawker, C. J. *J. Am. Chem. Soc.* **1994**, *116*, 11185.

(16) In the notation of block copolymers, *z* corresponds to the molar fraction of the functionality in the functionalized block only, and the M_n's given relate to the PS and functionalized-PS blocks in the corresponding parent polymer scaffold.

(17) Shenhar, R.; Sanyal, A.; Uzun, O.; Rotello, V. M. *Macromolecules* **2004**, *37*, 92.

(18) Ilhan, F.; Gray, M.; Blanchette, K.; Rotello, V. M. *Macromolecules* **1999**, *32*, 6159.

(19) Winnik, F. M. *Chem. Rev.* **1993**, *93*, 587.

(20) Winnik, F. M.; Tamai, N.; Yonezawa, J.; Nishimura, Y.; Yamazaki, I. *J. Phys. Chem.* **1992**, *96*, 1967.

(21) Farid, S.; Martic, P. A.; Daly, R. C.; Thompson, D. R.; Specht, D. P.; Hartman, S. E.; Williams, J. L. R. *Pure Appl. Chem.* **1979**, *51*, 241.

(22) Gray, M.; Cuello, A. O.; Cooke, G.; Rotello, V. M. *J. Am. Chem. Soc.* **2003**, *125*, 7882. Cooke, G.; Rotello, V. M. *Chem. Soc. Rev.* **2002**, *31*, 275. Niemz, A.; Rotello, V. M. *Acc. Chem. Res.* **1999**, *32*, 44.

(23) Katritzky, A. R.; Ghiviriga, I. *J. Chem. Soc., Perkin Trans. 2* **1995**, 1651.

(24) Beijer, F. H.; Sijbesma, R. P.; Vekemans, J. A. J.; Meijer, E. W.; Kooijman, H.; Spek, A. L. *J. Org. Chem.* **1996**, *61*, 6371.

(25) Donth, E. *The Glass Transition: Relaxation Dynamics in Liquids and Disordered Materials*; Springer: New York, 2001.

(26) Bicerano, J. *Prediction of Polymer Properties*, 3rd ed.; Marcel Dekker: New York, 2002.

(27) See, for example: Sunder, A.; Bauer, T.; Mulhaupt, R.; Frey, H. *Macromolecules* **2000**, *33*, 1330. Yuan, Y.; Shoichet, M. S. *Macromolecules* **1999**, *32*, 2669. Miyoshi, T.; Takegoshi, K.; Terao, T. *Macromolecules* **1999**, *32*, 8914. Dorr, M.; Zentel, R.; Dietrich, R.; Meerholz, K.; Brauchle, C.; Wichern, J.; Zippel, S.; Boldt, P. *Macromolecules* **1998**, *31*, 1454. Parthiban, A.; Le Guen, A.; Yansheng, Y.; Hoffmann, U.; Klapper, M.; Müllen, K. *Macromolecules* **1997**, *30*, 2238. Kuo, S.-W.; Kao, H.-C.; Chang, F.-C. *Polymer* **2003**, *44*, 6873. Xua, H.; Kuo, S.-W.; Lee, J.-S.; Chang, F.-C. *Polymer* **2002**, *43*, 5117. Wirasate, S.; Dhumrongvaraporn, S.; Allen, D. J.; Ishida, H. *J. Appl. Polym. Sci.* **1998**, *70*, 1299. Gao, H.; Harmon, J. P. *J. Appl. Polym. Sci.* **1998**, *64*, 507. He, C.; Griffin, A. C.; Windle, A. H. *J. Appl. Polym. Sci.* **1994**, *53*, 561. Dang, T. D.; Mather, P. T.; Alexander, M. D., Jr.; Grayson, C. J.; Houtz, M. D.; Spry, R. J.; Arnold, F. E. *J. Polym. Sci., Polym. Chem.* **2000**, *38*, 1991. Stengersmith, J. D.; Henry, R. A.; Hoover, J. M.; Lindsay, G. A.; Nadler, M. P.; Nissan, R. A. *J. Polym. Sci., Polym. Chem.* **1993**, *31*, 2899. Pellice, S. A.; Fasce, D. P.; Williams, R. J. J. *J. Polym. Sci., Polym. Phys.* **2003**, *41*, 1451. Barbeau, P.; Gerard, J. F.; Magny, B.; Pascault, J. P. *J. Polym. Sci., Polym. Phys.* **2000**, *38*, 2750. Schmaljohann, D.; Haussler, L.; Potschke, P.; Voit, B. I.; Loontjens, T. J. A. *Macromol. Chem. Phys.* **2000**, *201*, 49. Gestoso, P.; Brisson, J. *Comput. Theor. Polym. Sci.* **2001**, *11*, 263.

(28) *Physical Properties of Polymers Handbook*; Mark, J. E., Ed.; American Institute of Physics: Woodbury, NY, 1996.

(29) *Polymer Handbook*, 4th ed.; Brandrup, J., Immergut, E. H., Grulke, E. A., Eds.; Wiley-Interscience: New York, 1999.

(30) The slightly lower glass transition temperatures observed for the (28:13, 40%) block copolymers compared to the analogous (25, 50%) random copolymers is associated with the slightly lower functionality content in the block copolymers.[17]

(31) Strobl, G. *The Physics of Polymers*; Springer: Berlin, 1996.

(32) Doi, M. *Introduction to Polymer Physics*: Clarendon Press: Oxford, 1996.

(33) Jablonski, E. L.; Gorga, R. E.; Narasimhan, B. *Polymer* **2003**, *44*, 729. Gorga, R. E.; Jablonski, E. L.; Thiyagarajan, P.; Seifert, S.; Narasimhan, B. *J. Polym. Sci., Part B: Polym. Phys.* **2002**, *40*, 255. van Ekenstein, G. O. R. A.; Meyboom, R.; ten Brinke, G.; Ikkala, O. *Macromolecules* **2000**, *33*, 3752. Oudhuis, A. A. C. M.; ten Brinke, G.; Karasz, F. E. *Polymer* **1993**, *34*, 1991. Salomons, W.; ten Brinke, G.; Karasz, F. E. *Polym. Commun.* **1991**, *32*, 185.

(34) Vavasour, J. D.; Whitmore, M. D. *Macromolecules* **1992**, *25*, 5477.

(35) Leibler, L. *Macromolecules* **1980**, *13*, 1602.

(36) Matsen, M. W.; Bates, F. S. *Macromolecules* **1996**, *29*, 1091.

(37) Shull, K. R. *Macromolecules* **1992**, *25*, 2122. Olvera de la Cruz, M.; Mayes, A. M. *Macromolecules* **1991**, *24*, 3975.

(38) Helfand, E.; Wasserman, Z. R. *Macromolecules* **1976**, *9*, 879. Ohta, T.; Kawasaki, K. *Macromolecules* **1986**, *19*, 2621.

(39) Semenov, A. N. *Sov. Phys. JETP* **1985**, *61*, 733. Semenov, A. N. *Macromolecules* **1993**, *26*, 6617.

(40) Melenkevitz, J.; Muthukumar, M. *Macromolecules* **1991**, *24*, 4199.

(41) Hasegawa, H.; Tanaka, H.; Yamasaki, K.; Hashimoto, T. *Macromolecules* **1987**, *20*, 1651. Hashimoto, T.; Shibayama, M.; Kawai, H. *Macromolecules* **1980**, *13*, 1237.

(42) Ren, Y.; Lodge, T. P.; Hillmyer, M. A. *Macromolecules* **2000**, *33*, 866. Ren, Y.; Lodge, T. P.; Hillmyer, M. A. *Macromolecules* **2002**, *35*, 3889.

(43) The absence of distinct Bragg reflections in PS/DEP, PS/Anth, and PS/Pyr of the (27:13, 17%) composition does not arise from low electron density contrast, as PS/DAP(27:13, 17%) does exhibit a distinct reflection, while the calculated electron densities for all four functionalities vary within less than 2%.

(44) All precursors to polymers of series B were synthesized from the same batch of PS block, with the same styrene/CMS mixture composition (i.e., comonomer quantities); thus, the differences in length between the functionalized blocks of these polymers resulted only from different polymerization times.

(45) (a) Almdal, K.; Rosedale, J. H.; Bates, F. S.; Wignall, G. D.; Fredrickson, G. H. *Phys. Rev. Lett.* **1990**, *65*, 1112. (b) Hadziioannou, G.; Skoulios, A. *Macromolecules* **1982**, *15*, 258.

(46) Semiempirical calculations using topological indices (see Experimental Section and ref 17) estimate $\chi_{S,S-DAP}$ from solubility parameters by 0.58, which is within the same order of magnitude of that of the experimental determination.

(47) Ilhan, F.; Gray, M.; Rotello, V. M. *Macromolecules* **2001**, *34*, 2597.

(48) Markees, D. G. *J. Org. Chem.* **1964**, *29*, 3120.

(49) The larger values calculated for the functionalized styrenes compared to that of styrene are in accord with increased stiffness induced by the added bulk.

MA0495590